Caloz, Christophe; Sihvola, Ari

Electromagnetic Chirality, Part 1: The Microscopic Perspective [Electromagnetic Perspectives]

Published in:
IEEE Antennas and Propagation Magazine

DOI:
10.1109/MAP.2019.2955698

Published: 01/02/2020

Document Version
Peer-reviewed accepted author manuscript, also known as Final accepted manuscript or Post-print

Please cite the original version:
Caloz, C., & Sihvola, A. (2020). Electromagnetic Chirality, Part 1: The Microscopic Perspective [Electromagnetic Perspectives]. *IEEE Antennas and Propagation Magazine*, *62*(1), 58-71. Article 8982214.
https://doi.org/10.1109/MAP.2019.2955698

Electromagnetic Chirality, Part I: Microscopic Perspective

Christophe Caloz, *Fellow, IEEE,* and Ari Sihvola, *Fellow, IEEE*

***Abstract*—This paper is the first part of a two-part paper, with the second part being [1], presenting a bottom-up description of electromagnetic chirality, which occurs in materials composed of particles with structural handedness[1]. This part deals with the microscopic perspective of chirality. First, it highlights the three fundamental concepts related to chirality – mirror asymmetry, polarization rotation and magnetodielectric coupling – and points out the nontrivial interdependencies existing between them. Then, it lists a number of assumptions that pertain to the overall document. Next, it argues that metamaterials represent the most promising technology for chiral applications, and discusses their geometrical parameters, dipolar responses and electromagnetic polarizabilities. The following part compares two representative metaparticles that are complementarily related to chirality, namely the planar Omega particle and the twisted Omega, or helix, particle, shows that only the latter is mirror-asymmetric, and hence chiral, deduces from the mirror asymmetry criterion that chirality requires a voluminal geometry, and infers the magnetoelectric properties of the planar Omega and helix particles from their geometry. Finally, it recalls how to convert the microscopic dipole moments and polarizabilies into macroscopic polarization densities and susceptibilities to obtain a medium representation of a (meta)material structure. Upon this basis, the second part of the paper presents a macroscopic perspective of electromagnetic chirality and chiral materials.**

***Index Terms*—Chirality, optical activity, chiral media, materials and metamaterials, mirror asymmetry, polarization rotation, magnetoelectric coupling, bianisotropy, Tellegen and Pasteur media, polarizability and susceptibility dyadic tensors, spatial dispersion or nonlocality, parity conditions, temporal dispersion or nonlocality, circular birefringence and circular dichroism, reciprocal and nonreciprocal gyrotropy.**

I. Introduction

The term *chirality* comes from the Greek word χείρ, which means *hand*. It is the *geometric property* according to which an object is *mirror-asymmetric* or, equivalently, different from its image in a mirror, irrespectively to orientation. The etymology and definition of chirality may be understood by considering Fig. 1. The (mirror-plane) image of the right (resp. left) hand is *not* superimposable with the right (resp. left) hand itself, but rather with the left (resp. right) hand. So, the human hands are chiral [sic], with right or left *handedness*, and the right and left hands are called the enantiomers (from the Greek, έναντι: opposite, μέρος: other) of each other. The fact that hands are certainly the most common chiral things that we deal with on a daily basis justifies the etymology. However, many other things are chiral, such as amino-acids – see Fig. 2 – and tris(bipyridine)ruthenium(II) chloride (red crystalline salt) in chemistry, DNA and sugars in biochemistry, sea snails and ammonite fossils in biology, screws and helical antennas in engineering, and fusilli pasta and twisted pastry in food!

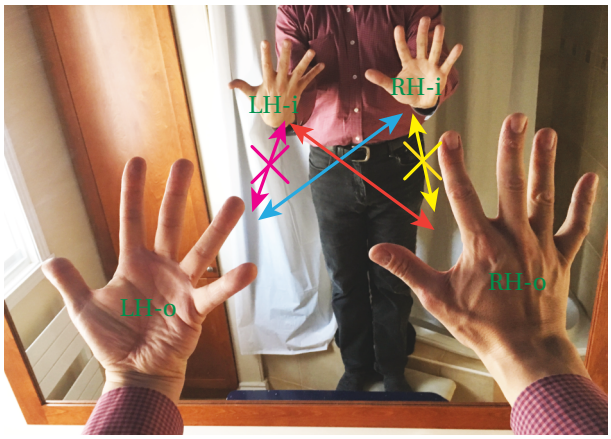

Fig. 1. Human hands and their reflection in a mirror. RH-o and LH-o are the original right hand (RH) and left hand (LH), while RH-i and LH-i are their images in the mirror, with the correspondence RH-o↔LH-i and LH-o↔RH-i. The non-superimposability may be specifically understood as follows. RH-i is finger-to-finger aligned with RH-o, but it shows its palm whereas RH-o shows its back. Flipping RH-i brings about back-to-back translational symmetry, but loses finger-to-finger symmetry. So, RH-i and RH-o are fundamentally different, irrespectively to their orientation in space. The same naturally applies to the pair (LH-o, LH-i). *(Photograph: Raphaël Caloz)*

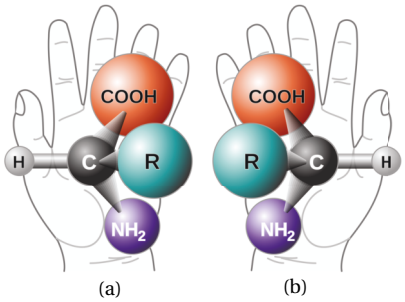

Fig. 2. Chirality in a generic amino acid (–NH_2: amine, –COOH: carboxyl, –R: rest of the molecule). (a) Left-handed (LH) enantiomer: with thumb along the C→H axis, it takes the left hand for the fingers to point from COOH to NH_2 through R. (b) Right-handed (RH) enantiomer: with thumb along the C→H axis, it takes the right hand for the fingers to point from COOH to NH_2 through R. *(Picture: Wikimedia Commons)*

[1]Recent papers use the terminology "chiral" to simply designate a wave that is circularly polarized and related effects [2], [3], particularly in the near-field and evanescent regimes with chirality parameter defined as $C = (\epsilon_0/2)\mathbf{E}\cdot\nabla\times\mathbf{E} + 1/(2\mu_0)\mathbf{B}\cdot\nabla\times\mathbf{B}$ or $C = -(\omega\epsilon_0/2)\mathrm{Im}\{\mathbf{E}^*\cdot\mathbf{B}\}$ [4], [5]. Although the geometrical locus formed by the tip of the electric (or magnetic) field vector of a circularly polarized wave indeed forms (in both space and time) a spiral, which is inherently a chiral shape, mere circular polarization does not correspond to what has been called 'chiral' in the past 200 years or so. For this reason, we find this terminology – according to which, incidentally, chirality would be all over the place in papers and books and antennas and optics – quite confusing, and we exclude it from this paper, where the term 'chiral' exclusively refers, as mentioned here, to phenomena occurring in "materials composed of particles with structural handedness."

A medium made of chiral molecules or particles is called a *chiral medium*. Such a medium has the remarkable property of rotating the polarization of electromagnetic waves propagating through it. This phenomenon of *polarization rotation*, also called *optical activity*, was first observed more than 200 years ago with light passing through 'translucent' substances by Arago in 1811 [6] and through quartz by Biot shortly later [7], and it was explained by Fresnel in terms of circular birefringence in 1821-22 [8]. It was further studied by Pasteur in salts of solutions of racemic mixtures[2] of tartrates near the middle of the XIX$^{\text{th}}$ century [9]. In 1898, Bose reported the first microwave observation of chiral polarization rotation, in twisted jute (fiber produced by some plants) structures [10], and, about twenty years later, Lindman introduced wire spirals as more practical artificial chiral particles [11]. In the course of the XX$^{\text{th}}$ century, it has been established that optical activity results from coupling between the electric and magnetic responses, or *magnetoelectric coupling*, of chiral particles, and different related form of electromagnetic constitutive relations have been proposed [12], [13], [14], [15], [16]. Towards the end of the century appeared the first textbooks on chiral and biisotropic media [17], [18].

Until the turn of the current century, chiral media had been mostly restricted to theoretical electromagnetic studies [17], [18], [19]. The advent of modern *metamaterials* (e.g. [20]) and, even more, *metasurfaces* (e.g. [21]) has dramatically changed the situation, and chiral media, along with their bianisotropic extension [19], have now become a practical reality that is poised to revolutionize microwave, terahertz and photonics technologies.

Chirality involves a number of concepts that are sometimes misunderstood and confused. These concepts include Pasteur and Tellegen biisotropy [18], biisotropy and bianisotropy [19], circular birefringence and circular dichroism [22], reciprocal and nonreciprocal polarization rotation [23], temporal and spatial electromagnetic symmetry [24], and temporal and spatial dispersion or nonlocality [24], [25]. This paper presents a global, intuitive and yet rigorous, first-principle description of chiral media and metamaterials. It is intended to serve as a self-consistent study document, as well as to dissipate misunderstandings and confusions, and hence help further research in the field.

The rest of this first part of the paper is organized as follows. Section II highlights the three fundamental concepts related to chirality – mirror asymmetry, polarization rotation and magnetodielectric coupling – and points out the nontrivial interdependencies existing between them. Section III lists a number of assumptions that pertain to the overall paper. Section IV argues that metamaterials represent the most promising technology for chiral applications, and discusses their geometrical parameters, dipolar responses and electromagnetic polarizabilities. Section V compares two representative metaparticles that are complementarily related to chirality, namely the planar Omega particle and the twisted Omega, or helix, particle and infers their magnetoelectric properties of from their geometry. As a transition to the second part [1], Sec. VI recalls how to convert the microscopic dipole moments and polarizabilies into macroscopic polarization densities and susceptibilities to obtain a medium representation of a metamaterial structure. Finally, Sec. VII enumerates the main conclusions of this part.

II. Preliminary Comment: the Chiral Trinity

Section I has pointed out that chirality is intimately related to the concepts of mirror asymmetry, polarization rotation and magnetoelectric coupling. Mirror asymmetry is today's geometrical definition of chirality, polarization rotation [or optical activity, or gyrotropy (Greek γῦρος: circle and τροπος: turn)] is the fundamental chiral effect on light observed two centuries ago by Arago and Biot, and magnetoelectric coupling (or, generally, bianisotropy) has been found to be a fundamental electromagnetic feature of chiral media in the course of the past century.

However, these concepts are not systematically interdependent, and it is of crucial importance to distinguish the relations existing between them. These relations are represented in Fig. 3, and will be demonstrated throughout the paper. They are the following:

- Mirror asymmetry is a necessary and sufficient conditions for chirality (❶). This requires no proof since the former is the definition of the latter, and the two may thus be considered as merged together[3].
- Mirror asymmetry implies both polarization rotation (②) and magnetoelectric coupling (③), but neither polarization rotation (④) nor electromagnetic coupling (⑤) implies mirror asymmetry.
- Polarization rotation does not imply magnetoelectric coupling (⑥), and magnetolectric coupling does not imply polarization rotation (⑦).

III. Global Assumptions

The following assumptions hold throughout the overall (two-part) paper:

1) All the media are *linear* and *time-invariant* (LTI).
2) They are excited by waves with *harmonic time dependence*, and *steady-state conditions* are assumed.
3) Due to 1) and 2), the electromagnetic responses of the media, and hence all the fields involved, have the same time dependence, and may thus be generally written versus space ($\mathbf{r}$) and time (t) in the elliptical polarization form

$$\mathcal{F}(\mathbf{r},t) = \mathbf{F}_1 \cos[\omega t - \phi(\mathbf{r})] + \mathbf{F}_2 \sin[\omega t - \phi(\mathbf{r})], \qquad (1)$$

where $\mathbf{F}_1$ and $\mathbf{F}_2$ are real perpendicular vectors, with circular polarization if $|\mathbf{F}_1| = |\mathbf{F}_2|$, and where ω is the temporal angular frequency ($\omega = 2\pi f$, f : frequency) and $\phi(\mathbf{r})$ is the spatial phase.
4) As implicitly assumed in 3), scalar and vector quantities are denoted by regular and bold characters,

[2] A racemic mixture is a mixture with an equal number of LH and RH particles, whose antagonistic chiral effects cancel out at the macroscopic scale.

[3] Note that a racemic mixture (see Footnote 2) is macroscopically mirror-symmetric, and hence achiral, while being microscopically (at the level of its individual constituent particles) mirror-asymmetric, and hence chiral.

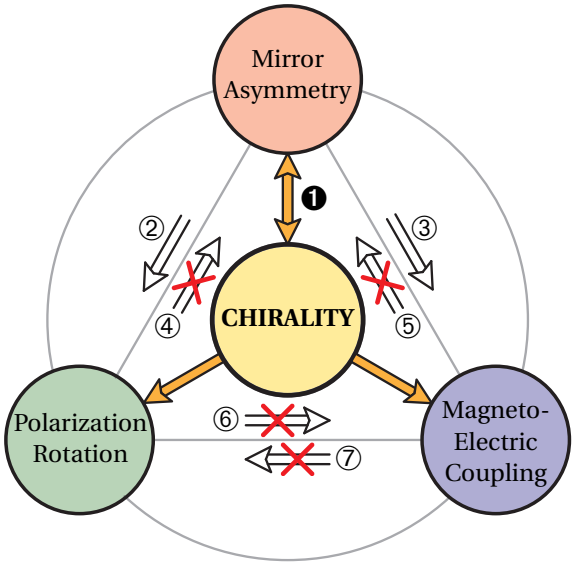

Fig. 3. The chiral trinity with implication relations between the three fundamentally related concepts of mirror asymmetry, polarization rotation and magnetoelectric coupling. The arrows indicate implications and the barred arrows indicate nonimplications.

respectively, while tensors are denoted by a double overline, as for instance $\overline{\overline{\chi}}$.

5) Given 3), we use the customary *phasor notation*, which conveniently allows to drop the time dependence in most calculations. The phasor corresponding to (1) is the auxiliary complex vector

$$\mathbf{F}(\mathbf{r}) = (\mathbf{F}_1 + i\mathbf{F}_2)\, \mathrm{e}^{i\phi(\mathbf{r})}. \tag{2}$$

6) The field (1) is then retrieved from (2) via the operation

$$\mathcal{F}(\mathbf{r}, t) = \mathrm{Re}\left\{\mathbf{F}(\mathbf{r})\mathrm{e}^{-i\omega t}\right\}, \tag{3}$$

where the physical field and its phasor are distinguished by calligraphic and regular characters, respectively.

7) The complex harmonic time dependence $\mathrm{e}^{-i\omega t}$ in (3) corresponds to the convention that is generally adopted in the physics community [19], [24]. The engineering community rather uses the equivalent convention $\mathrm{e}^{+j\omega t}$ [26], [27], where $j = -i$. We choose here the former convention because it is more common in the literature on complex media.

8) If the medium is *isotropic*, it is convenient to select a coordinate system that coincides with the direction of propagation, $\hat{\mathbf{k}}$. Here, assuming $\hat{\mathbf{k}} = \hat{\mathbf{z}}$, we therefore choose $\hat{\mathbf{r}} = \hat{\mathbf{z}}$. The corresponding phasor has the plane-wave form

$$\mathbf{F}(z) = (\mathbf{F}_1 + i\mathbf{F}_2)\, \mathrm{e}^{\pm i\beta z}, \tag{4}$$

which is related to (2) by $\phi(\mathbf{r}) = \phi(z) = \pm\beta z$ ($\beta = k = 2\pi/\lambda$, λ: wavelength). The corresponding complex spacetime function is $\mathrm{e}^{i(\pm\beta z - \omega t)}$, and the phase velocity is found by monitoring a wave point of fixed phase – i.e., $\partial(\pm\beta z - \omega t)/\partial t = \pm\beta\partial z/\partial t - \omega = 0$ – as $v_\mathrm{p} = \partial z/\partial t = \pm\omega/\beta \gtrless 0$ ($\beta > 0$), indicating that the positive and negative signs in (4) correspond to wave propagation in the $+z$ (forward) and $-z$ (backward) directions, respectively. Note that the choice of the plane-wave form in (4) is not restrictive since any wave in an LTI medium can be decomposed in a spectrum of plane waves from Fourier theory [28].

9) The sourceless time-harmonic Maxwell-Faraday and Maxwell-Ampère equations for the chosen $\mathrm{e}^{-i\omega t}$ time dependence are

$$\nabla \times \mathbf{E} = i\omega\mathbf{B}, \tag{5a}$$

$$\nabla \times \mathbf{H} = -i\omega\mathbf{D}, \tag{5b}$$

where $\mathbf{E}$ (V/m), $\mathbf{H}$ (A/m), $\mathbf{D}$ (C/m^2 = As/m^2) and $\mathbf{B}$ (Wb/m^2 = Vs/m^2) are the usual electric field, magnetic field, electric flux density (or displacement field), and magnetic flux density (or magnetic induction field), respectively, and $\mathbf{J}$ (A/m^2) is the electric current density.

IV. Metamaterial Implementation

A. Motivation and Definition

Although chiral molecules and substances, such as amino acids and sugars [18], [29], are abundant in nature, they are generally not amenable to electromagnetic applications, due to their chemical instability, high loss and/or restricted spectrum. Artificial chirality, in the form of metamaterials, is a much more promising avenue in this regard, since one can engineer chiral metamaterials with high robustness, low loss, arbitrary operation frequency and tailorable properties (e.g. [30], [31], [32], [33]).

A metamaterial is a medium constituted of a 1D, 2D or 3D subwavelength-lattice array of scattering particles – or 'metaparticles' – whose key properties are due more to the geometry and orientation of these particles than to the molecular-scale nature of the materials that compose them. Figure 4 shows an example of a 3D chiral metamaterial constituted of multiturn-helix-shaped metaparticles.

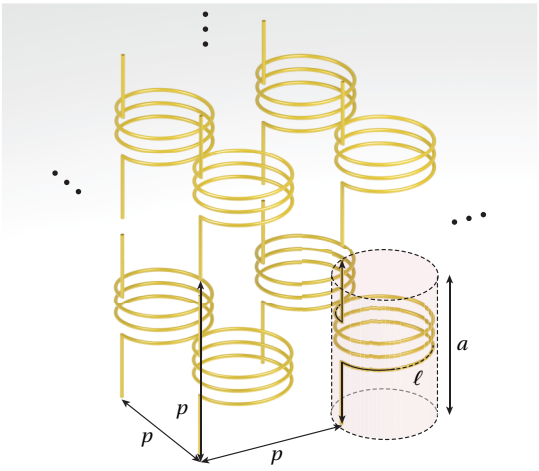

Fig. 4. Example of a 3D chiral metamaterial with significant dimensional parameters. Here the lattice is periodic with a cubic unit cell of dimension p, and it is made of multiturn-helix metaparticles of external size a and unfolded (resonant, $\sim \lambda_\mathrm{res}/2$) length ℓ, with $a \ll \ell$ [Eq. (8)].

B. Dimensional Constraints

The subwavelength-lattice array condition is necessary for the structure to be *homogeneizable*, and hence to really operate as a medium, without spurious diffraction and with well-defined constitutive parameters. Denoting the lattice feature (or period in the most common case of a periodic – crystal-like – structure) p, and the size of the metaparticle a, one must thus satisfy the relation

$$|k|a \leqslant |k|p \ll 2\pi \quad \text{or} \quad a \leqslant p \ll \lambda. \tag{6}$$

At the same time, to interact with an incoming wave, and hence transform that wave according to specifications, the metaparticle must be operated close to its resonance, which occurs at the frequency where its *resonant size*, ℓ, is about half the wavelength[4], i.e.,

$$\ell \approx \lambda_{\text{res}}/2. \tag{7}$$

Note that in the case of a metamaterial, one invariably uses this halfwavelength (or first or lowest) resonance ($m = 1$ in $\ell \approx m\lambda_{\text{res}}/2$), because higher resonances would imply larger metaparticle electric sizes, which opposes the fundamental homogeneizable medium requirement (6).

The conditions (6) and (7) are clearly antagonistic, since a and ℓ are both related to the size of the metaparticle. Fortunately, the 'external size', which we define as the size of the smallest box fully containing the particle, i.e., here a, can be made substantially smaller than the resonant size, ℓ, by folding an initially simple (e.g. straight or single-looped) structure of dimension ℓ upon itself in the three directions of space, as illustrated in Fig. 4, and by leveraging reactive (inductive and capacitive) loading, which ultimately leads to the viable and typical metamaterial regime

$$a \leqslant p \ll \ell \approx \lambda_{\text{res}}/2 < \lambda_{\text{res},0}, \tag{8}$$

where λ represents the wavelength of the wave in the possibly dielectric medium that embeds or surrounds (e.g. supporting substrate) the particle and λ_0 represents the wavelength of the wave in free space ($\lambda < \lambda_0$). Figure 4 illustrates Eq. (6), with $\lambda = \lambda_0$ if the particles stand in free-space, and $\lambda < \lambda_0$ if they include material loads or are supported by a dielectric matrix frame. Typical metamaterials involve parameters in the order of $a \in [\lambda_0/15 - \lambda_0/4]$ and $p = \in [\lambda_0/12 - \lambda_0/4]$ [20].

C. Metaparticle Selection

As regular materials owe their macroscopic properties to their constitutive atoms and molecules, metamaterials owe their macroscopic properties to their metaparticles. Since they are deeply subwavelength, these metaparticles are restricted to *dipolar responses*[5], characterized by the electric dipole moment $\mathbf{p}_{\text{e}}$ (Asm) and by the magnetic dipole moments $\mathbf{p}_{\text{m}}$ (Vsm), which are respectively defined as [24], [25]

$$\mathbf{p}_{\text{e}} = \int_V \mathbf{r}'\rho(\mathbf{r}')d\mathbf{r}', \tag{9a}$$

$$\mathbf{p}_{\text{m}} = \mu_0\mathbf{m} = \frac{\mu_0}{2}\int_V \mathbf{r}' \times \mathbf{J}(\mathbf{r}')d\mathbf{r}', \tag{9b}$$

where $\rho(\mathbf{r})$ and $\mathbf{J}(\mathbf{r})$ are the spatial distributions of the electric charge density and current density, respectively, and where the volume integration corresponds to the structure of the particle. Note that we have here redefined the usual magnetic dipole moment $\mathbf{m}$ [24] as $\mathbf{p}_{\text{m}} = \mu_0\mathbf{m}$ for symmetry in the forthcoming chiral relations. In a simple artificial-dielectric metamaterial, the electric dipolar response ($\mathbf{p}_{\text{e}}$) is exclusively due to the electric excitation ($\mathbf{E}$), and we denote it here $\mathbf{p}_{\text{ee}}$, while the magnetic dipolar response ($\mathbf{p}_{\text{m}}$) is exclusively due to the magnetic excitation ($\mathbf{H}$), and we denote it here $\mathbf{p}_{\text{mm}}$. The best particle for ($\mathbf{p}_{\text{ee}}$) is a straight conducting wire or a straight dielectric rod, according to Maxwell-Faraday law, in the microwave and optical regimes, respectively, while the best particle for ($\mathbf{p}_{\text{mm}}$) is a looped conducting wire or a looped dielectric rod, according to Maxwell-Ampère law. A combined $\mathbf{p}_{\text{ee}}$–$\mathbf{p}_{\text{mm}}$ particle leads then generally to a Lorentz-dispersive composite positive/negative-index metamaterial [34], with negative index [35] below the electric and magnetic plasma frequencies and positive index above [20], as will be shown in [1].

However, as mentioned in Sec. I and as will be seen later, chirality is fundamentally related to a magnetoelectric response within the chiral particle. The most natural strategy to realize such a coupled response is to structurally merge the aforementioned straight and looped elements into a 'single-block' particle, so that conduction or displacement current continuity in the resulting block adds $\mathbf{p}_{\text{em}}$ to $\mathbf{p}_{\text{ee}}$ and $\mathbf{p}_{\text{me}}$ to $\mathbf{p}_{\text{mm}}$. Such a single-block straight-looped metaparticle could look like the particles that are shown in Fig. 5, with straight and looped sections of respective lengths $2d$ and s, summing up to the unfolded length ℓ and interrelated from (7) as

$$\ell = 2d + s \approx \frac{\lambda_{\text{res}}}{2}, \tag{10a}$$

$$\text{i.e.,} \quad s \approx \frac{\lambda_{\text{res}}}{2} - 2d \quad \text{or} \quad d \approx \frac{\lambda_{\text{res}}}{4} - \frac{s}{2}. \tag{10b}$$

Equation (10b) reveals that the straight- and looped-section lengths are *antagonistic* to each other, an observation that will be seen in [1] to be of great importance in the response and design of chiral metamaterials.

D. Metaparticle Polarizabilities

As the atoms and molecules in regular materials, the metaparticles in a metamaterial may be conveniently characterized in terms of *polarizabilities* [24], [36]. In the case of a general metamaterial, involving anisotropy and magneto-electric coupling, such characterization may be expressed in terms of the electric dipole moments and magnetic dipole moments induced by the electric and magnetic fields as

$$\begin{pmatrix} \mathbf{p}_{\text{ee}} & \mathbf{p}_{\text{em}} \\ \mathbf{p}_{\text{me}} & \mathbf{p}_{\text{mm}} \end{pmatrix} = \begin{pmatrix} \overline{\overline{\alpha}}_{\text{ee}} \cdot \mathbf{E}_{\text{loc}} & \overline{\overline{\alpha}}_{\text{em}} \cdot \mathbf{H}_{\text{loc}} \\ \overline{\overline{\alpha}}_{\text{me}} \cdot \mathbf{E}_{\text{loc}} & \overline{\overline{\alpha}}_{\text{mm}} \cdot \mathbf{H}_{\text{loc}} \end{pmatrix} \tag{11}$$

[4] The exact resonance length may somewhat deviate from half the wavelength due to reactive loading effects caused by the folding of the particle onto itself (e.g. see Fig. 4)

[5] In general, a multipole expansion is required for modeling the scattering from an object [24]. However, the multipoles of order larger than the dipoles have a negligible effect when the object is deeply subwavelength, as is the case for a metaparticle, according to (8).

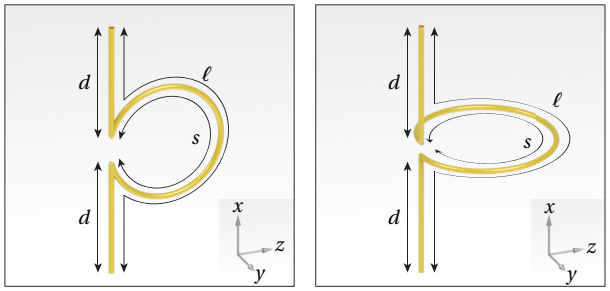

Fig. 5. Two metaparticles with merged straight and looped sections, that are complementarily related to chirality. (a) Planar Omega particle. (b) Twisted Omega or helix particle (single-turn version of the helix in Fig. 4).

where $\overline{\overline{\alpha}}_{ee}$, $\overline{\overline{\alpha}}_{em}$, $\overline{\overline{\alpha}}_{me}$ and $\overline{\overline{\alpha}}_{mm}$ are the electric-to-electric, magnetic-to-electric, electric-to-magnetic and magnetic-to-magnetic 3×3 coupling dyadic tensors, respectively, which are measured in $\mathrm{Asm^2/V}$, $\mathrm{sm^2}$, $\mathrm{sm^2}$ and $\mathrm{Vsm^2/A}$ (see Appendix A), and where $\mathbf{E}_{loc}$ and $\mathbf{H}_{loc}$ are the local excitation fields. Figure 6 details the notation used in this paper for the components of the polarizability tensors in a Cartesian coordinate system. The local excitation fields are the difference between the global excitation fields and the fields produced by the polarization of the neighboring particles in a dense medium [24], [29], and reduce to the excitation fields, **E** and **H**, in a sufficiently dilute medium. The paper assumes that the dilute-medium approximation is valid, until the final design guidelines at the end of [1], which does not represents a significant restriction for qualitative description.

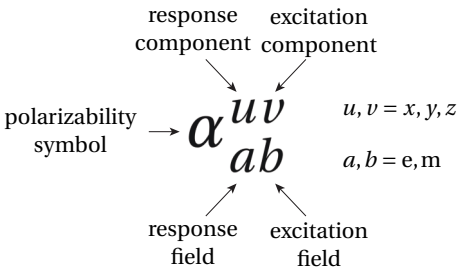

Fig. 6. Notation for the components of the polarizability dyadic tensors in Eq. (11), and susceptibility dyadic tensors to appear farther, in a Cartesian coordinate system. Here, the excitation fields are considered to be **E** and **H**, and the responses are the vectorial dipole moments $\mathbf{p}_e$ and $\mathbf{p}_m$ corresponding respectively to the response fields **D** and **B** in the medium formed by these moments (see Sec. VI). The polarizability may be most efficiently read out as "u-directed a response due to v-directed b excitation." For instance, α_{em}^{xy} is the polarizability component corresponding to the x-directed electric response due to a y-directed magnetic excitation, or to the polarization p_{e,H_y}^{x}.

V. Two Metaparticle Study Cases

A. Mirror-Symmetry Test

According to the rationale in Sec. IV-C, the planar and twisted straight/looped-section metaparticles, which are respectively shown in Figs. 5(a) and 5(b), are both potential candidates for chiral particles, because they both involve magnetoelectric coupling, as we shall show in Secs. V-C and V-D. However, as we shall see, such coupling is only a necessary condition for chirality, the absolute (necessary and sufficient condition) criterion being mirror asymmetry (Sec. II) according to the definition of Sec. I. Let us then apply the mirror test, depicted in Fig. 7, to the two metaparticles.

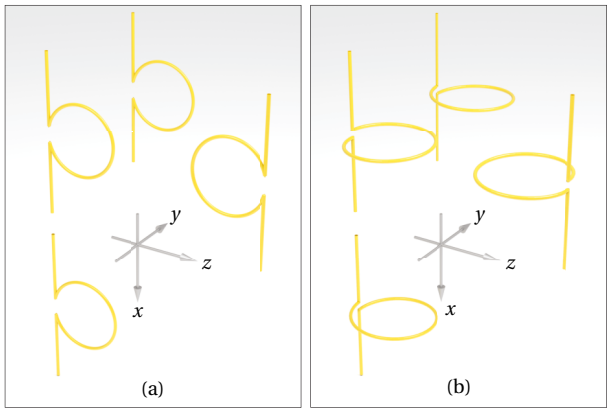

Fig. 7. Mirror reflections of the two particles in Fig. 5. (a) Planar Omega particle [Fig. 5(a)] (lying here in the xz plane), which is mirror-symmetric and hence not chiral. (b) Twisted Omega or helix particle [Fig. 5(b)] (extending in the 3 directions space), which is mirror-asymmetric, and hence chiral. The original particle in the left top is RH, whereas its three images are LH.

Let us start with the planar Omega particle [Fig. 5(a)], tested in Fig. 7(a). Upon reflection in the x, y and z directions, this particle transforms into images that are exactly identical to itself. The z-direction image is flipped in space, but can be flipped back, without any structural change, to perfectly superimpose with the original particle, and is hence indeed also identical to it. So, the particle is identical to any of its mirror images. Therefore, it is not chiral or, equivalently, has no handedness. It should therefore not induce any polarization rotation, as shall be verified in Sec. V-C.

How about the twisted Omega or helix particle [Fig. 5(b)], tested Fig. 7(b)? This particle differs from its planar counterpart only by the 90° twist of the loop section with respect to the straight section. However, this twist, which assigns it a voluminality, plays a determinant role in the mirror test: the three images are now different from the original particle; they are LH whereas the original one is RH. So, the twisted Omega particle, as the human hand (Fig. 1), is chiral, and we shall see in Sec. V-D that it possesses the consequently expected polarization rotation property[6].

Despite the fact that the planar Omega particle is not chiral, we shall still analyze it in the sequel of this section, as its comparison with the twisted Omega or helix particle is instructive for a deep understanding of chirality.

[6]If the z-mirrored helix particle were next y-mirrored, it would naturally flip handedness again, and hence retrieve the original RH handedness. However, such a double-reflection operation ($z\to-z$ followed by $y\to-y$) does not correspond to a reflection in the xy direction but to a rotation of 180° about the x axis. In contrast, yet an additional reflection along x would yield again, as a single reflection, the reverse (LH) handedness. This is because a triple reflection along x, y and z ($z\to-z$, $y\to-y$, $x\to-x$) is equivalent to a single reflection in the xyz direction ($\mathbf{r}\to-\mathbf{r}$).

B. Volume Necessary (but Insufficient) Condition

Comparing Fig. 5(b) with Fig. 5(a) shows that the RH helix particle is obtained by twisting the planar particle about the z axis in the clockwise direction, as a key in a lock to open a door, whereas the LH helix particle is obtained by twisting the planar particle about the z axis in the counterclockwise direction, as to close a door. So, the voluminal twist has imparted handedness, and hence chirality, to the particle.

Such 'handedness-ization' would not have been possible without transforming the initially planar structure into a voluminal one. Indeed, a volume-less, purely planar structure, such as the planar Omega particle, looks indeed identical from its two sides, and the existence of nonplanarity or volume, as in the helix particle or the hand (Fig. 1), is clearly necessary for handedness[7], that allows handedness. So, a particle must necessarily include a volume, or thickness, or depth, to be chiral. Moreover, the smallest dimension of this volume must be a significant fraction of the wavelength for a significant chiral effect, since either the electric dipole from the wire section or the magnetic dipole from loop section could otherwise be to weak in regard of the required amount of magnetoelectricity.

However, three-dimensionality is only a necessary condition – and not a sufficient condition! – for chirality. An obvious proof of the latter insufficiency is the case of a spherical particle. Transforming the planar Omega particle into a volume particle by adding to it untwisted looped sections about the x axis (e.g. in the xz plane) also does not make the particle different from its mirror image and hence chiral.

C. Planar Omega Particle (Achiral)

The $\mathbf{p}_{\mathrm{ee,em}}$ and $\mathbf{p}_{\mathrm{me,mm}}$ dipolar responses of the planar Omega particle, which is now known Sec. V-A to be achiral from, are depicted in Fig. 8, where the particle lies in the xz plane with its straight section directed along x. Let us separately examine the responses to the electric part (top of the figure) and magnetic part (bottom of the figure) of the electromagnetic field excitation to separately determine the electric-response and magnetic-response polarizability pairs $(\overline{\overline{\alpha}}_{\mathrm{ee}}, \overline{\overline{\alpha}}_{\mathrm{em}})$ and $(\overline{\overline{\alpha}}_{\mathrm{me}}, \overline{\overline{\alpha}}_{\mathrm{mm}})$.

An x-directed electric field excitation induces an x-directed electric dipole moment p^{x}_{e,E_x} in the straight section of the particle, which corresponds to the electric-to-electric polarizability $\alpha^{xx}_{\mathrm{ee}}$. The current associated with this dipole moment must then flow in the loop section, due to current continuity, and this occurs in the same (upward in the figure) direction given the subwavelength, $\lambda/2$-dimension of the unfolded particle [Eq. (8)]. This looped current gives rise to the y-directed magnetic dipole moment p^{y}_{m,E_x}, which corresponds to the electric-to-magnetic polarizability $\alpha^{yx}_{\mathrm{me}}$. Due to symmetry and due to the subwavelength size of the loop, scattering from the z-oriented parts of this (looped) current cancels out, and hence does not produce any $\alpha^{zx}_{\mathrm{ee}}$; in contrast, scattering from its x-oriented parts does not cancel out, due to the asymmetry induced by the gap, and therefore slightly contribute as $\alpha^{xx}_{\mathrm{ee}}$.

[7] If the hand had no thickness, it would reduce to its mere projection, and hence have neither a palm nor a back. It would therefore look identical from both sides, and have thus no handedness!

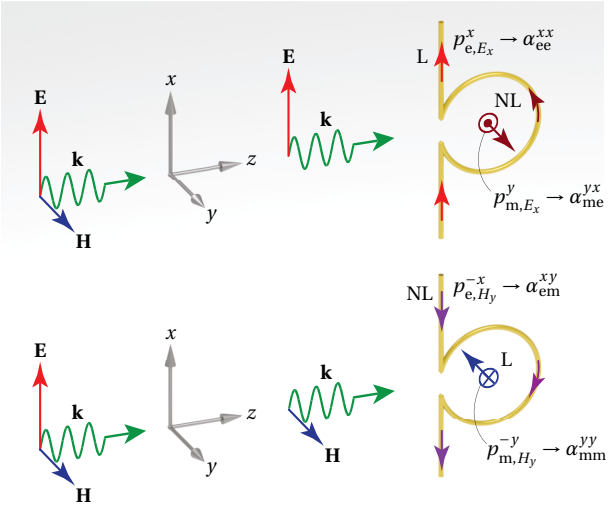

Fig. 8. Electromagnetic response of the planar Omega particle (achiral) to plane-wave excitation. The top and bottom represent the response to the electric and magnetic parts, respectively, of the electromagnetic field excitation. Only the polarization case corresponding to nonzero polarizabilities (polarization E_x–H_y) is shown here. Using (10), one may evaluate the length of each of the straight sections, d, and the circumference of the loop, s to $d \approx \lambda/10$ and $s \approx 3\lambda/10$.

The response to the magnetic field is found by a symmetric reasoning. A y-directed magnetic field excitation induces a y-directed magnetic dipole moment p^{-y}_{m,H_y} in the direction opposing the incident field (Lenz law) in the looped section of the particle, which corresponds to the magnetic-to-magnetic polarizability $\alpha^{yy}_{\mathrm{mm}}$. Due to the same symmetry reason as before, the associated looped current produces a small $\alpha^{xy}_{\mathrm{em}}$ response but no $\alpha^{zy}_{\mathrm{em}}$ response. The looped current must then flow along the straight sections, due to current continuity, and this occurs in the same (downward in the figure) direction given the subwavelength, $\lambda/2$-dimension of the unfolded particle. This straight current gives rise to the x-directed electric dipole moment p^{-x}_{e,H_y}, which corresponds to the main part of the magnetic-to-electric polarizability $\alpha^{xy}_{\mathrm{em}}$.

Note that the polarizabilities $\alpha^{yx}_{\mathrm{me}}$ and $\alpha^{xy}_{\mathrm{em}}$ must have the same magnitude since they involve the same geometrical parts without involving any nonreciprocity [23]. However, they are oppositely directed. Therefore,

$$\alpha^{yx}_{\mathrm{me}} = -\alpha^{xy}_{\mathrm{em}}. \tag{12a}$$

Upon considering the other two Cartesian orientations of the particle in Fig. 8, as further discussed later, this relation generalizes to the tensorial relation

$$\bar{\bar{\alpha}}_{\mathrm{me}} = -\bar{\bar{\alpha}}^{\mathrm{T}}_{\mathrm{em}}, \tag{12b}$$

where the superscript T denotes the transpose operation. Equation (12b) is an expression of the *Onsager microscopic reversibility principle* [37], [38] applied here to a meta-particle: in the absence of an external time-reversal anti-symmetric influence, such as for instance a magnetic field or an electric current [24], any process is microscopically

reversible, and hence reciprocal, with the magnetodielectric reciprocity condition (12b) [23]).

One may easily verify that the E_x–H_y polarization considered in Fig. 8 is the only one that produces nonzero polarizabilities, assuming that the conductor forming the particle has a deeply-subwavelength, and hence negligible, diameter[8]. The global susceptibility tensors of the planar Omega particle in Fig. 8 are then [39]

$$\begin{pmatrix} \overline{\overline{\alpha}}_{\rm ee} & \overline{\overline{\alpha}}_{\rm em} \\ \overline{\overline{\alpha}}_{\rm me} & \overline{\overline{\alpha}}_{\rm mm} \end{pmatrix} = \begin{pmatrix} \begin{pmatrix} \alpha_{\rm ee}^{xx} & 0 & 0 \\ 0 & 0 & 0 \\ 0 & 0 & 0 \end{pmatrix} \begin{pmatrix} 0 & \alpha_{\rm em}^{xy} & 0 \\ 0 & 0 & 0 \\ 0 & 0 & 0 \end{pmatrix} \\ \begin{pmatrix} 0 & 0 & 0 \\ -\alpha_{\rm em}^{xy} & 0 & 0 \\ 0 & 0 & 0 \end{pmatrix} \begin{pmatrix} 0 & 0 & 0 \\ 0 & \alpha_{\rm mm}^{yy} & 0 \\ 0 & 0 & 0 \end{pmatrix} \end{pmatrix}. \tag{13}$$

The tensor (13) can be modified by transforming the 'monoatomic' metaparticle of Fig. 8(a) into a 'biiatomic' metaparticle or 'triatomic' metaparticle, obtained by adding copies of the initial particle (here in the xz or zx plane) in the other two or three planes. This can be done in a diversity of ways. In each plane, the planar Omega particle can take one out of 4 distinct orientations: the straight section can be directed along the two perpendicular directions of the plane and for each of these orientations the looped section may point to two opposite directions. This may be best seen by using proper labeling. For instance, the particle of Fig. 8(a) may be labeled $(zx,x,+z)$, indicating that it is lying in the zx plane, with straight section in the x direction and looped section pointing towards the $+z$ direction, and the same plane supports also the three other orientations $(zx,x,-z)$, $(zx,z,+x)$ and $(zx,z,-x)$. There are then $4^1=4$ possibilities for a monoatomic particle, $4^2=16$ possibilities for a biatomic particle, and $4^3=64$ possibilities for a triatomic particle.

The triatomic particle formed by to the cyclic permutations of the particle in Fig. 5(a), i.e., $[(zx,x,+z),(xy,y,+x),(yz,z,+y)]$, can be easily found, by the same permutations, to correspond to the metaparticle tensors

$$\begin{pmatrix} \overline{\overline{\alpha}}_{\rm ee} & \overline{\overline{\alpha}}_{\rm em} \\ \overline{\overline{\alpha}}_{\rm me} & \overline{\overline{\alpha}}_{\rm mm} \end{pmatrix} = \begin{pmatrix} \alpha_{\rm ee}\overline{\overline{I}} & \alpha_{\rm em}\overline{\overline{I}}_{\rm P} \\ \alpha_{\rm me}\overline{\overline{I}}_{\rm P}^{\rm T} & \alpha_{\rm mm}\overline{\overline{I}} \end{pmatrix}, \tag{14}$$

where $\overline{\overline{I}}$ and $\overline{\overline{I}}_{\rm P}$ are the symmetric and post-permutated unit tensors $\overline{\overline{I}}=\hat{\mathbf{x}}\hat{\mathbf{x}}+\hat{\mathbf{y}}\hat{\mathbf{y}}+\hat{\mathbf{z}}\hat{\mathbf{z}}$ and $\overline{\overline{I}}_{\rm P}=\hat{\mathbf{x}}\hat{\mathbf{y}}+\hat{\mathbf{y}}\hat{\mathbf{z}}+\hat{\mathbf{z}}\hat{\mathbf{x}}$, respectively. In such a metaparticle, the direct (ee and mm) tensors have reduced to scalar, but the cross (em and me) tensors have not, so that the overall response is still anisotropic.

[8] If the diameter measures a substantial fraction of the wavelength, small responses would also exist in the other directions, leading to extra tensorial components. One could then approximate the different sections by straight and looped ellipsoids, and specifically prolate spheroids with large (needle-type) axis ratio. For instance, if the aspect ratio is $10:1$, the polarizability of a straight needle reads $\alpha=V\epsilon_0(\epsilon_{\rm r}-1)/[1+K(\epsilon_{\rm r}-1)]=V\epsilon_0/K$, assuming that it is perfectly conducting ($\epsilon_{\rm r}\to i\infty$), where V is the volume of the needle, ϵ_0 the free-space permittivity, and K the depolarization factor in the direction considered. For an x-oriented needle, the depolarization factors are found to be $K_x=0.02$ and $K_y=K_z=0.49$ [29]. Hence there exists polarizability components perpendicular to the needle axis, but they are $0.49/0.02=24.5$ smaller than that along the axis, and may thus be neglected. So, for sections with a length-to-diameter ratio of more than 10, such effects can be safely ignored.

The most 'symmetric' nontrivial medium that can be obtained with the the planar Omega particle is in fact the hexatomic medium with the particles $(zx,x,+z)$ and $(yz,y,+z)$ providing the components $\hat{\mathbf{z}}\times\overline{\overline{I}}$ [see Eq. (13) for $(zx,x,+z)$], $(xy,y,+x)$ and $(zx,z,+x)$ providing $\hat{\mathbf{x}}\times\overline{\overline{I}}$, and $(xy,x,+y)$ and $(yz,z,+y)$ providing $\hat{\mathbf{y}}\times\overline{\overline{I}}$. The corresponding polarizability tensors may be written

$$\begin{pmatrix} \overline{\overline{\alpha}}_{\rm ee} & \overline{\overline{\alpha}}_{\rm em} \\ \overline{\overline{\alpha}}_{\rm me} & \overline{\overline{\alpha}}_{\rm mm} \end{pmatrix} = \begin{pmatrix} \alpha_{\rm ee}\overline{\overline{I}} & \alpha_{\rm em}\overline{\overline{I}}_{\rm A} \\ \alpha_{\rm me}\overline{\overline{I}}_{\rm A} & \alpha_{\rm mm}\overline{\overline{I}} \end{pmatrix}, \tag{15}$$

where $\overline{\overline{I}}_{\rm A}$ is the (6-component) antisymmetric tensor $\overline{\overline{I}}_{\rm A}=\mathbf{r}\times\overline{\overline{I}}$. However, such a metaparticle involves 2 particles per plane, which tends to conflict with the dimensional constraint (8).

Note that allowing more than one planar Omega particle per plane may also wash out the magnetoelectric coupling effects of the resulting multiatomic metaparticle. For instance, if the zy plane were allowed to support the $(zx,x,-z)$ particle in addition to the $(zx,x,+z)$ particle in Fig. 8, then the responses $\alpha_{\rm me}^{yx}$ and $\alpha_{\rm em}^{xy}$ would disappear due to cancelation of the scattering from the two particles. The hexaomic metaparticle obtained by adding the two complementary cancelling pairs would lead then to a magnetoelectic-less structure.

How about polarization rotation? We have seen above that, for the polarization in Fig. 8, the electric response of the metaparticle is fully parallel to the electric excitation ($\mathbf{p}_{\rm ee}\|\mathbf{E}$ and $\mathbf{p}_{\rm em}\|\mathbf{E}$) and the magnetic response is fully parallel to the magnetic excitation ($\mathbf{p}_{\rm me}\|\mathbf{H}$ and $\mathbf{p}_{\rm mm}\|\mathbf{H}$), despite coupling, as also clearly apparent in (13), (14) and (15). This means that the particle does not induce any rotation for this polarization; it only induces a phase shift, ϕ_x, corresponding to its interaction with the wave. However, the problem is actually more subtle. Consider now the polarization $\mathbf{E}\|\hat{\mathbf{y}}$ in Fig. 8. In this case, the particle does essentially not interact with the wave and is hence invisible to it; so, there is again no rotation, and $\phi_y=0$. But this *phase birefringence* (different phase responses for different polarizations) of the particle actually alters the polarization direction of *obliquely polarized* waves, since it differently affects their x and y components. However, this effect is a waveplate-type polarization modification [40][9] rather than the polarization rotation or gyrotropic effect occurring in a chiral medium.

In summary, we have found that the planar Omega particle in Fig. 8 has the following properties:

[9] With the phase birefringence $(\phi_x,\phi_y)=(\phi_x,0)$, a linearly polarized oblique incident wave $\boldsymbol{\mathcal{E}}^{\rm i}=\mathrm{Re}\{(\hat{\mathbf{x}}+\hat{\mathbf{y}})e^{-i\omega t}\}=\cos(\omega t)(\hat{\mathbf{x}}+\hat{\mathbf{y}})$ is transmitted across the particle as $\boldsymbol{\mathcal{E}}^{\rm t}=\mathrm{Re}\{\mathbf{E}^{\rm t}e^{-i\omega t}\}=\mathrm{Re}\{(e^{i\phi_x}\hat{\mathbf{x}}+\hat{\mathbf{y}})e^{-i\omega t}\}=\cos(\omega t-\phi_x)\hat{\mathbf{x}}+\cos(\omega t)\hat{\mathbf{y}}$, which corresponds to an elliptically polarized wave; in the particular case $\phi_x=\pi/2$, we have $\boldsymbol{\mathcal{E}}^{\rm t}=\mathrm{Re}\{(i\hat{\mathbf{x}}+\hat{\mathbf{y}})e^{-i\omega t}\}=\sin(\omega t)\hat{\mathbf{x}}+\cos(\omega t)\hat{\mathbf{y}}$, which corresponds to a quarter-wave plate, where the incident linear polarization is transformed into circular polarization (and vice-versa). The reader may easily verify that the other particular case $\phi_x=\pi$ (still with $\phi_x=0$) corresponds to a half-wave plate, where the incident linear polarization is transformed into a perpendicular linear polarization while an incident circular polarization is transformed into a circular polarization of the opposite handedness.

1) It indeed involves magnetoelectric coupling, as predicted in Sec. IV-C, since $\overline{\overline{\alpha}}_{\rm em}, \overline{\overline{\alpha}}_{\rm me} \neq 0$, which is the reason it was called pseudo-chiral in [39], and $\overline{\overline{\alpha}}_{\rm me} = -\overline{\overline{\alpha}}_{\rm em}$;
2) Despite such coupling, it is strictly achiral, by definition, since it is identical to its mirror image, as shown in Sec. V-A (proof of ⑤ in Fig. 3);
3) It cannot reduce to an isotropic particle upon adding copies in the other two directions of space.
4) As expected from its achiral nature (Sec. I) and despite its magnetoelectric coupling, it does not involve polarization rotation (proof of ⑦ in Fig. 3), and his hence not gyrotropic.

D. Twisted Omega or Helix Particle (Chiral)

The $\mathbf{p}_{\rm ee,em}$ and $\mathbf{p}_{\rm me,mm}$ dipolar responses of the twisted Omega or helix particle, which is now known from Sec. V-A to be chiral, are depicted in Fig. 9, where the straight section is directed along x, while the loop section lies in the yz plane. Let us again separately examine the responses to the electric part (top of the figure) and magnetic part (bottom of the figure) of the electromagnetic field excitation to separately determine the electric-response and magnetic-response polarizability pairs $(\overline{\overline{\alpha}}_{\rm ee}, \overline{\overline{\alpha}}_{\rm em})$ and $(\overline{\overline{\alpha}}_{\rm me}, \overline{\overline{\alpha}}_{\rm mm})$.

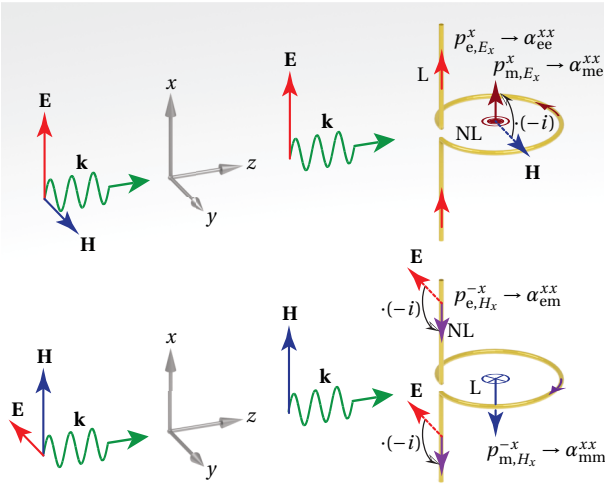

Fig. 9. Electromagnetic response of the twisted Omega or helix (here RH) particle (chiral) to plane-wave excitation. The top and bottom represent the responses to the electric and magnetic parts, respectively, of the electromagnetic field excitation. Only the polarization cases corresponding to nonzero polarizabilities are shown (polarizations E_x–H_y and $-E_y$–H_x). The dimensional comment in the caption of Fig. 8 also holds here.

An x-directed electric field excitation induces again an x-directed electric dipole moment $p^x_{{\rm e},E_x}$ on the straight section of the particle, corresponding to $\alpha^{xx}_{\rm ee}$, and the current associated with this dipole moment again flows in the loop section from current continuity. However, given the 90° twist of the loop, this current now gives rise to the x-directed magnetic dipole moment $p^x_{{\rm m},E_x}$, which corresponds to $\alpha^{xx}_{\rm me}$. Note in passing the if the angle of the loop twist were not exactly 90° – e.g. 60° – then the induced magnetic moment would be tilted, which would introduce parasitic off-axis contributions to the response. Moreover, an x-directed magnetic field excitation (different form the y-directed one at the bottom of Fig. 8) induces an x-directed magnetic dipole moment $p^{-x}_{{\rm m},H_x}$ in the looped section of the particle, corresponding to $\alpha^{xx}_{\rm mm}$, plus, from current continuity, the x-directed electric dipole moment $p^{-x}_{{\rm e},H_y}$, corresponding to $\alpha^{xx}_{\rm em}$. Again, the cross polarizations are opposite, i.e.,

$$\alpha^{xx}_{\rm me} = -\alpha^{xx}_{\rm em}, \tag{16a}$$

generalizing as (12a) to

$$\bar{\bar{\alpha}}_{\rm me} = -\bar{\bar{\alpha}}^{\rm T}_{\rm em}. \tag{16b}$$

In addition, the looped current produces the responses $\alpha^{yx}_{\rm ee}$ and $\alpha^{yx}_{\rm em}$ (without $\alpha^{zx}_{\rm ee}$ and $\alpha^{zx}_{\rm em}$) due to the gap asymmetry; however, these responses are negligibly small as the yz plane projection of the gap is very small and may even reach zero, and we therefore henceforth consider them negligible.

So, the four main susceptibilities identified above correspond to the dyadic component xx. The helix metaparticle in Fig. 9 has thus the polarizability tensors

$$\begin{pmatrix} \overline{\overline{\alpha}}_{\rm ee} & \overline{\overline{\alpha}}_{\rm em} \\ \overline{\overline{\alpha}}_{\rm me} & \overline{\overline{\alpha}}_{\rm mm} \end{pmatrix} = \begin{pmatrix} \begin{pmatrix} \alpha^{xx}_{\rm ee} & 0 & 0 \\ 0 & 0 & 0 \\ 0 & 0 & 0 \end{pmatrix} \begin{pmatrix} \alpha^{xx}_{\rm em} & 0 & 0 \\ 0 & 0 & 0 \\ 0 & 0 & 0 \end{pmatrix} \\ \begin{pmatrix} -\alpha^{xx}_{\rm em} & 0 & 0 \\ 0 & 0 & 0 \\ 0 & 0 & 0 \end{pmatrix} \begin{pmatrix} \alpha^{xx}_{\rm mm} & 0 & 0 \\ 0 & 0 & 0 \\ 0 & 0 & 0 \end{pmatrix} \end{pmatrix}, \tag{17}$$

and the 'triatomic' metaparticle formed by adding copies of that particle in the y and z directions, as shown in Fig. 10, has the polarizability tensors

$$\begin{pmatrix} \overline{\overline{\alpha}}_{\rm ee} & \overline{\overline{\alpha}}_{\rm em} \\ \overline{\overline{\alpha}}_{\rm me} & \overline{\overline{\alpha}}_{\rm mm} \end{pmatrix} = \begin{pmatrix} \alpha_{\rm ee}\overline{\overline{I}} & \alpha_{\rm em}\overline{\overline{I}} \\ -\alpha_{\rm em}\overline{\overline{I}} & \alpha_{\rm mm}\overline{\overline{I}} \end{pmatrix}, \tag{18}$$

which have this time reduced to scalars and are thus *isotropic*. Remarkably, and in contrast with the 64 possibilities of the straight Omega particle, this arrangement the helix particle is unique[10]! In this sense, the helix particle is much more symmetric and fundamental than the planar Omega particle.

In fact, magnetoelectricity automatically follows from mirror asymmetry. Mirror asymmetry implies some structural voluminal twist, as in the helical particle studied here, and such a twist necessarily leads to magnetoelectric coupling since it brings about current continuity between noncoplanar straight and loop parts. In fact, even just the (voluminal) twisted loop part of the particle in Fig. 9 without the vertical parts involves magnetoelectric coupling, despite a very low strength due to the smallness of the vertical (electrical dipole) projections of the loop. Thus, mirror asymmetry implies magnetoelectric coupling (proof of ③ in Fig. 3).

[10]This, of course, assumes only one type of handedness, either RH or LH. If we allow both LH and RH particles, we have $2^3 = 8$ possible combinations (2 handednesses in each of the 3 directions of space). However, 6 of these combinations lead to different signs in different directions, which breaks biisotropy. The arrangement of Fig. 10 – and its LH counterpart whose χ has the opposite sign – are the only ones yielding purely scalar polarizabilities, or biisotropy.

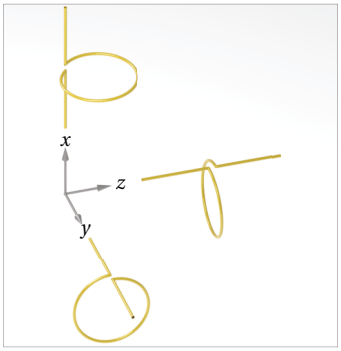

Fig. 10. 'Triatomic' (RH) metaparticle from by the combination of (RH) helical metaparticles (Fig. 9) oriented in the three directions of space.

Let us now see how chirality implies polarization rotation. Indeed, we have now, along with $\mathbf{p}_{\mathrm{ee}} \| \mathbf{E}$ and $\mathbf{p}_{\mathrm{mm}} \| \mathbf{H}$, that $\mathbf{p}_{\mathrm{me}} \perp \mathbf{H}$ and $\mathbf{p}_{\mathrm{em}} \perp \mathbf{E}$ (Fig. 9), indicating that part of the electromagnetic field has been rotated by 90°, corresponding to the expected polarization rotation. Specifically, the initially $+y$-directed field $\mathbf{H}$ (top of the figure) has rotated towards the $+x$ direction into p^{x}_{m,E_x}, while the initially $-y$-directed field $\mathbf{E}$ (bottom of the figure) has rotated towards the $-x$ direction into p^{-x}_{e,H_x}. The electromagnetic field has therefore rotated about the z axis in the direction corresponding to the left-hand with the thumb pointing in the propagation direction $(+z)$[11]. In other words, the field phasors associated with the cross coupling terms have rotated by the angle of $-\pi/2$ (y to x direction) or, equivalently, have been multiplied by the factor $\mathrm{e}^{-i\pi/2} = -i$, and therefore the cross coupling polarizabilities are in quadrature with their direct coupling counterparts. A LH particle naturally leads to rotation in the opposite direction.

In contrast to the planar Omega particle (Fig. 8), the twisted Omega or helix particle involves two different polarization states in its nonzero polarizabilities. Specifically, in Fig. 9, the polarization (E_x, H_y) involves $\alpha^{xx}_{\mathrm{ee}}$ and $\alpha^{xx}_{\mathrm{me}}$, while the polarization $(-E_y, H_x)$ involves $\alpha^{xx}_{\mathrm{mm}}$ and $\alpha^{xx}_{\mathrm{em}}$. In the case of a circularly polarized exciting wave, these two states are separated by the time interval $T/4$ ($T = \omega/(2\pi)$: time period) of the harmonic wave, which correspond to a factor $\mathrm{e}^{-i\pi/2} = -i$ in phasor notation.

These observations indicate mirror asymmetry necessarily induces polarization rotation (proof of ② in Fig. 3).

In summary, we have found that the twisted Omega or helix particle in Fig. 8 has the following properties:

1) It indeed involves magnetoelectric coupling, as predicted in Sec. IV-C, since $\overline{\overline{\alpha}}_{\mathrm{em}}, \overline{\overline{\alpha}}_{\mathrm{me}} \neq 0$, and $\overline{\overline{\alpha}}_{\mathrm{me}} = -\overline{\overline{\alpha}}_{\mathrm{em}}$;
2) It is chiral, by definition, since it is different to its mirror image, as shown in Sec. V-A and allowed by its volume configuration (Sec. V-B);
3) It reduces to an isotropic particle upon adding copies in the other two directions of space, corresponding to a purely diagonal polarizability response.
4) As expected from its chiral nature (Sec. I), it induces polarization rotation, i.e., it is gyrotropic.
5) The polarizability pairs $(\alpha^{xx}_{\mathrm{ee}}, \alpha^{xx}_{\mathrm{me}})$ and $(\alpha^{xx}_{\mathrm{mm}}, \alpha^{xx}_{\mathrm{em}})$ are in a quadrature relationship.

Analytical formulas for the polarizabilities of the helix particle in terms of its geometrical parameters are given in [41]. Alternative chiral particles may be inferred from the *voluminal twist* requirement noted in this section. It is important to note that the voluminality condition disqualifies all purely planar particles; even twisted purely planar particles, such as swastika crosses, are achiral[12]. However, chiral particles may take alternative shapes, such as their multiturn-helix, or spring, version in Fig. 4, the square-loop version of the helix in Fig. 5 – possibly in quasi-planar configuration with twist voluminality provided by conducting vias or swastika-type with twist voluminality provided by displacement current (see Appendix B) – or more complex structures looking like the amino acids represented in Fig. 2.

VI. Microscopic-to-Macroscopic Scales Conversion

Section IV-D has shown that metaparticles can be characterized by polarizability tensors, according to the relation (11), and Secs V-C and V-D have shown how to determine the structure of these tensors for the planar Omega particle and for the twisted Omega or helix particle, respectively. Arranging copies of such particles in the three dimensions of space, either randomly or according to a crystal-like lattice, and under the dimensional constraints outlined in Sec. IV-B, forms a metamaterial, as described in Sec. IV-A. This section outlines the conversion from the *microscopic* scale of the metaparticles to the *macroscopic* scale of the corresponding metamaterial.

As previously mentioned, we assume here dilute metamaterials, i.e. metamaterials with relatively low metaparticle density, and hence negligible inter-particle coupling. This assumption is often not valid, particularly in metamaterials leveraging tight inter-particle coupling for broad operational bandwidth [34]. However, it is acceptable to understand the essence of chirality, and it may be relaxed by including interaction tensors [42] and overcome by full-wave analysis, as will be seen in [1].

Under the aforementioned assumption of negligible inter-particle interaction, the microscopic electric and magnetic dipole moments $\mathbf{p}_{\mathrm{ee,em}}$ and $\mathbf{p}_{\mathrm{me,mm}}$ can be simply averaged in space and orientation to provide the corresponding macroscopic electric and magnetic polarization densities, $\mathbf{P}_{\mathrm{e}}$ (As/m^2) and $\mathbf{P}_{\mathrm{m}} = \mu_0 \mathbf{M}$ (Vs/m^2), where $\mathbf{M}$ is the usual magnetization [24], [29], [36], from which the medium properties follow. This leads here to the relations

$$\begin{aligned}\mathbf{P}_{\mathrm{e}} &= N\langle \mathbf{p}_{\mathrm{e}} \rangle = N\big(\langle \mathbf{p}_{\mathrm{ee}} \rangle + \langle \mathbf{p}_{\mathrm{em}} \rangle\big) = N\Big(\langle \overline{\overline{\alpha}}_{\mathrm{ee}} \cdot \mathbf{E} \rangle + \langle \overline{\overline{\alpha}}_{\mathrm{em}} \cdot \mathbf{H} \rangle\Big) \\ &= N\Big(\langle \overline{\overline{\alpha}}_{\mathrm{ee}} \rangle \cdot \mathbf{E} + \langle \overline{\overline{\alpha}}_{\mathrm{em}} \rangle \cdot \mathbf{H}\Big), \end{aligned} \tag{19a}$$

[11] In contrast to the planar Omega particle, the twisted Omega particle alters all the linear polarization states in a similar fashion, since the rotation effect is found for the two orthogonal polarizations in Fig. 9.

[12] Such structures have a kind of handedness, corresponding to the direction of the bends, but this is a weak form of handedness since it depends on the observation direction, so that the particles are identical to their mirror image and hence do not support gyrotropy (see Appendix B).

$$\mathbf{P}_{\rm m} = N\langle \mathbf{p}_{\rm m}\rangle = N\big(\langle \mathbf{p}_{\rm em}\rangle + \langle \mathbf{p}_{\rm mm}\rangle\big) = N\Big(\langle \overline{\overline{\alpha}}_{\rm me}\cdot\mathbf{E}\rangle + \langle \overline{\overline{\alpha}}_{\rm mm}\cdot\mathbf{H}\rangle\Big)$$
$$= N\Big(\langle \overline{\overline{\alpha}}_{\rm me}\rangle\cdot\mathbf{E} + \langle \overline{\overline{\alpha}}_{\rm mm}\rangle\cdot\mathbf{H}\Big), \tag{19b}$$

where the $\langle\cdot\rangle$ symbol represents the averaging operation, N ($1/\mathrm{m}^3$) denotes the particle density, and the other quantities were defined in Secs. IV-C and IV-D. Consistently with the negligible inter-particle coupling assumption, we have dropped the subscript 'loc' that appeared in (11) (see Sec. IV-D) in the second equalities, and considered the metaparticles to be aligned according to a lattice with well-defined coordinate system in the third equalities.

The particle average densities of polarizabilities in (19) are related to the medium *susceptibilities*, $\overline{\overline{\chi}}_{ab}$, as

$$N\langle \overline{\overline{\alpha}}_{\rm ab}\rangle = c_{ab}\overline{\overline{\chi}}_{ab}, \tag{20a}$$

with the normalizing factors

$$c_{\rm ee} = \epsilon_0, \quad c_{\rm em} = c_{\rm em} = \sqrt{\epsilon_0\mu_0}, \quad c_{\rm mm} = \mu_0, \tag{20b}$$

where $\epsilon_0 = 8.854\cdot 10^{-12}$ As/Vm and $\mu_0 = 4\pi\cdot 10^{-7}$ Vs/Am are the free-space permittivity and permeability, respectively [24], [29], [36]. Substituting (20) into (19) transforms these relations into

$$\mathbf{P}_{\rm e} = \epsilon_0\overline{\overline{\chi}}_{\rm ee}\cdot\mathbf{E} + \sqrt{\epsilon_0\mu_0}\,\overline{\overline{\chi}}_{\rm em}\cdot\mathbf{H}, \tag{21a}$$
$$\mathbf{P}_{\rm m} = \sqrt{\epsilon_0\mu_0}\,\overline{\overline{\chi}}_{\rm me}\cdot\mathbf{E} + \mu_0\overline{\overline{\chi}}_{\rm mm}\cdot\mathbf{H}, \tag{21b}$$

where $\overline{\overline{\chi}}_{\rm ee}$, $\overline{\overline{\chi}}_{\rm em}$, $\overline{\overline{\chi}}_{\rm me}$ and $\overline{\overline{\chi}}_{\rm mm}$ are the (unitless) electric-to-electric, magnetic-to-electric, electric-to-magnetic and magnetic-to-magnetic susceptibility dyadic tensors, respectively, whose notation follows the conventions in Fig. 6.

VII. Conclusions

In the first part of this two-part paper, we have presented a microscopic description of electromagnetic chirality and materials. The main conclusions and results of this part may be summarized as follows:

1) Chirality is a geometric property according to which an object is mirror-asymmetric or, equivalently, different from its image in a mirror, irrespectively to orientation.
2) As a consequence of 1), a chiral particle must have a volume; a purely planar particle is always mirror symmetric, and therefore never chiral. In addition, the particle must include some structural twisting. Volumic twisting is a necessary and sufficient condition for chirality.
3) A (biisotropic) chiral material or metamaterial is a medium constituted of chiral particles or metaparticles oriented in the three directions of space (e.g. the triatomic chiral particle in Fig. 10). Such a medium induces polarization rotation (irrespectively to the polarization of the incident wave), associated with magnetoelectric coupling (coupling between the electric and magnetic responses).
4) According to 1) and 3), chirality is intimately related to the concepts of mirror asymmetry, polarization rotation and magnetoelectric coupling. However, these concepts are not trivially interdependent:
   - According to 1), mirror asymmetry is a necessary and sufficient condition for chirality.
   - Mirror asymmetry implies polarization rotation and magnetoelectric coupling, but neither polarization rotation nor magnetoelectric coupling implies mirror asymmetry.
   - Polarization rotation and magnetoelectric coupling do not imply each other.
5) In a (reciprocal) magnetoelectric particle, the electric-to-magnetic and magnetic-to-electric responses are always opposite to each other.
6) A planar – and hence achiral – particle involving magnetoelectric coupling, such as the planar Omega particle studied in the paper, cannot be combined to form an isotropic medium; the resulting medium is necessarily bianisotropic (and achiral). In contrast, a chiral particle, such as the helix particle studied in the paper, can, assuming a triatomic metaparticle with a copy of the basic chiral particle in each of the three directions of space (or a random arrangement of such copies).
7) What is conventionally called a 'chiral medium' in the chiral community is the isotropic (or biisotropic) chiral medium, but a chiral medium (with mirror asymmetry, and hence magnetoelectric coupling and polarization rotation) can of course also be anisotropic, i.e. birefringently anisotropic, with chiral particles only along one or two directions of space.

The concepts and results of this first part will be naturally extended in the second part of the paper, which will deal with the macroscopic description and properties of electromagnetic chirality and materials [43].

Acknowledgment

The three-dimensional drawings of the particles in the figures have been realized by Amar Al-Bassam, using the 3D computer graphics software Blender.

References

[1] C. Caloz and A. Sihvola, "Electromagnetic chirality, Part II: Macroscopic perspective," *IEEE Antennas Propag. Mag.* to be published.
[2] Y. Tang and A. E. Cohen, "Optical chirality and its interaction with matter," *Phys. Rev. Lett.*, vol. 104, pp. 163901:1–4, Apr. 2010.
[3] K. Y. Bliokh and F. Nori, "Characterizing optical chirality," *Phys. Rev. A*, vol. 83, no. 2, pp. 021803:1–3, 2011.
[4] E. Hendry, T. Carpy, J. Johnston, M. Popland, R. V. Mikhaylovskiy, A. J. Lapthorn, S. M. Kelly, L. D. Barron, N. Gadegaard, and M. Kadodwala, "Ultrasensitive detection and characterization of biomolecules using superchiral fields," *Nature Technol.*, vol. 5, pp. 783–787, Oct. 2010.
[5] T. J. Davis and E. Hendry, "Superchiral electromagnetic fields created by surface plasmons in nonchiral metallic nanostructures," *Phys. Rev. B*, vol. 87, pp. 085405:1–5, Jun. 2013.
[6] D. F. J. Arago, "Mémoire sur une modification remarquable qu'éprouvent les rayons lumineux dans leur passage à travers certains corps diaphanes et sur quelques autres nouveaux phénomènes d'optique," *Ann. Chem. Phys.*, vol. 2, no. 9, pp. 372–389, 1812. Mémoire présenté le 11 août 1811.
[7] J.-B. Biot, *Mémoires sur un nouveau genre d'oscillation que les molécules de la lumière éprouvent en traversant certains cristaux.* Chez Firmin Didot, 1814.
[8] A. Fresnel, *Oeuvres Complètes d'Augustin Fresnel.* Imprimerie impériale, 1868. Vol. 1:731-51; vol. 2:479-596.
[9] L. Pasteur, *Recherches sur les propriétés spécifiques des deux acides qui composent l'acide racémique.* Impr. Bachelier, 1850.

[10] J. C. Bose, "On the rotation of plane of polarization of electric waves by twisted structure," *Proc. Royal Soc.*, vol. 63, pp. 146–152, Jan. 1898.

[11] K. F. Lindman, "Om en genom ett isotropt system av spiralformiga resonatorer alstrad rotationspolarisation av de elektromagnetiska vågorna," *Öfversigt af Finska Vetenskaps-Societetens förhandlingar, A*, vol. 57, no. 3, pp. 1–32, 1914.

[12] E. U. Condon, "Theories of optical rotatory power," *Rev. Modern Phys.*, vol. 9, pp. 432–457, Oct. 1937.

[13] B. D. H. Tellegen, "The gyrator, a new electric network element," *Philips Res. Rep.*, vol. 3, pp. 81–101, Apr. 1948.

[14] E. J. Post, *Formal Structure of the Electromagnetics*. North-Holland, 1962.

[15] J. A. Kong, "Theorems of bianisotropic media," *Proc. IEEE*, vol. 60, pp. 1036–1046, Sep. 1972.

[16] F. I. Fedorov, *Teoria Girotropii*. Nauka i Technika, 1976.

[17] A. Lakhtakia, V. K. Varadan, and V. V. Varadan, *Time-harmonic Electromagnetic Fields in Chiral Media*, vol. 335. Springer, 1989.

[18] I. V. Lindell, A. H. Sihvola, S. A. Tretyakov, and A. J. Viitanen, *Electromagnetic Waves in Chiral and Bi-Isotropic Media*. Artech, 1994.

[19] J. A. Kong, *Electromagnetic Wave Theory*. EMW Publishing, 2008.

[20] F. Capolino, ed., *Metamaterials Handbook*. CRC Press, 2009. 2 volumes.

[21] K. Achouri and C. Caloz, "Design, concepts, and applications of electromagnetic metasurfaces," *Nanophotonics*, vol. 7, pp. 1095–1116, Jun. 2018.

[22] M. Born and E. Wolf, *Principles of Optics: Electromagnetic Theory of Propagation, Interferance and Diffraction of Light*. Cambridge University Press, seventh ed., 1999.

[23] C. Caloz, A. Alù, S. Tretyakov, D. Sounas, K. Achouri, and Z.-L. Deck-Léger, "Electromagnetic nonreciprocity," *Phys. Rev. Appl.*, vol. 10, pp. 047001:1–26, Oct. 2018.

[24] J. D. Jackson, *Classical Electrodynamics*. Wiley, third ed., 1998.

[25] L. D. Landau, L. P. Pitaevskii, and E. M. Lifshitz, *Electrodynamics of Continuous Media*, vol. 8 of *Course of theoretical physics*. Butterworth-Heinemann, second ed., 1984. Chap. XII.

[26] R. F. Harrington, *Time-Harmonic Electromagnetic Fields*. McGraw-Hill, 1961.

[27] D. M. Pozar, *Microwave Engineering*. Wiley, fourth ed., 2011.

[28] P. C. Clemmow, *The Plane Wave Spectrum Representation of Electromagnetic Fields*. The IEEE/OUP Series on Electromagnetic Wave Theory, IEEE Press, 1996. classical reissue.

[29] A. H. Sihvola, *Electromagnetic Mixing Formulas and Applications*. IET, 1999.

[30] G. Kenanakis, E. N. Economou, C. Soukoulis, and M. Kafesaki, "Controlling THz and far-IR waves with chiral and bianisotropic metamaterials," *EPJ Applied Metamaterials*, vol. 2, pp. 15:1–12, 2015.

[31] Z. Wang, F. Cheng, T. Winsor, and Y. Liu, "Optical chiral metamaterials: a review of the fundamentals, fabrication methods and applications," *Nanotechnology*, vol. 27, pp. 412001:1–20, Sep. 2016.

[32] X. Ma, M. Pu, X. Li, Y. Guo, P. Gao, and X. Luo, "Meta-chirality: fundamentals, construction and applications," *Nanomaterials*, vol. 7, no. 5, pp. 116:1–17, 2017.

[33] M. Qiu, L. Zhang, Z. Tang, W. Jin, C.-W. Qiu, and D. Y. Lei, "3d metaphotonic nanostructures with intrinsic chirality," *Adv. Funct. Mater.*, vol. 28, pp. 1803147:1–16, Nov. 2018.

[34] C. Caloz and T. Itoh, *Electromagnetic Metamaterials: Transmission Line Theory and Microwave Applications*. Wiley and IEEE Press, 2005.

[35] R. A. Shelby, D. R. Smith, and S. Schultz, "Experimental verification of a negative index of refraction," *Science*, vol. 292, pp. 77–79, Apr. 2001.

[36] A. Ishimaru, *Electromagnetic Wave Propagation, Radiation, and Scattering: From Fundamentals to Applications*. Wiley - IEEE Press, second ed., 2017.

[37] L. Onsager, "Reciprocal relations in irreversible processes I," *Phys. Rev.*, vol. 37, p. 405–426, Feb. 1931.

[38] L. Onsager, "Reciprocal relations in irreversible processes II," *Phys. Rev.*, vol. 38, p. 2265–2279, December 1938.

[39] S. M. I. Saadoun and N. Engheta, "A reciprocal phase shifter using novel pseudochiral or ω medium," *Microw. Opt. Technol. Lett.*, vol. 5, pp. 184–188, Apr. 1992.

[40] B. E. A. Saleh and M. C. Teich, *Fundamentals of Photonics*. Wiley-Interscience, second ed., 2007.

[41] S. A. Tretyakov, F. Mariotte, C. R. Simovski, T. G. Kharina, and J.-P. Heliot, "Analytical antenna model for chiral scatterers: comparison with numerical and experimental data," *IEEE Tran. Antennas Propag.*, vol. 44, pp. 1006–1014, Jul. 1996.

[42] R. E. Collin, *Field Theory of Guided Waves*. Wiley-IEEE Press, second ed., 1990. Chap. 12: "Artificial Dielectrics".

[43] C. Caloz and A. Sihvola, "Electromagnetic chirality, Part I: Microscopic perspective," *IEEE Antennas Propag. Mag.*, 2019. to be published.

Appendix A
Units of the Polarizabilities

The units of the polarizabilities in the dipole moment expressions (11) may be found as

$$\left[\overline{\overline{\alpha}}_{\rm ee}\right] = \left[\frac{\mathbf{p}_{\rm ee}}{\mathbf{E}_{\rm loc}}\right] = \frac{\rm Asm}{\rm V/m} = \frac{\rm Asm^2}{\rm V}, \tag{22a}$$

$$\left[\overline{\overline{\alpha}}_{\rm em}\right] = \left[\frac{\mathbf{p}_{\rm em}}{\mathbf{H}_{\rm loc}}\right] = \frac{\rm Asm}{\rm A/m} = \rm sm^2, \tag{22b}$$

$$\left[\overline{\overline{\alpha}}_{\rm me}\right] = \left[\frac{\mathbf{p}_{\rm me}}{\mathbf{E}_{\rm loc}}\right] = \frac{\rm Vsm}{\rm V/m} = \rm sm^2, \tag{22c}$$

$$\left[\overline{\overline{\alpha}}_{\rm mm}\right] = \left[\frac{\mathbf{p}_{\rm mm}}{\mathbf{H}_{\rm loc}}\right] = \frac{\rm Vsm}{\rm A/m} = \frac{\rm Vsm^2}{\rm A}. \tag{22d}$$

Appendix B
Planar-Technology Metaparticles

Chiral metaparticles may be implemented in planar or quasi-planar technology. The voluminality condition (Sec. V-B) is then provided by stacking structural – typically conducting – layers in a dielectric substrate configuration with the layers being interconnected either by conduction currents or displacement currents.

Figure 11 shows a planar-technology chiral metaparticle of the first kind, where the connections between the planar structural layers are realized by *conduction currents* flowing along vertical (x-direction in the figure) metalized via holes. Such particles are essentially 'planarized' versions of the helix metaparticles in Figs. 4 and 5(b), and are hence essentially explained by Sec. IV. They may then be randomly or triatomically (i.e., using a unit cell of the type shown in Fig. 10) arranged in three-dimensional space. Although their structure is quasi-planar, the resulting chiral metamaterial is really three-dimensional.

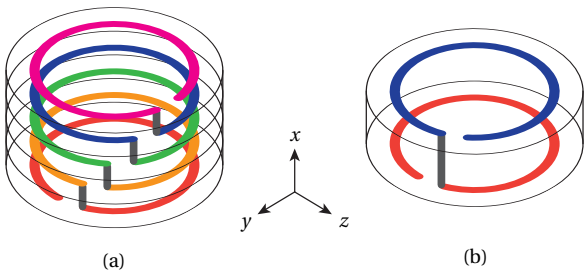

Fig. 11. Planar-technology helix-type chiral (LH) metaparticles for three-dimensional chiral metamaterials. (a) Five-layer structure. (b) Two-layer structure.

Figure 12 shows a planar-technology chiral metaparticle of the second kind, where the connections between the planar structural layers are realized by *displacement currents*, as will be shown next. The mirror test of Fig. 1 reveals that the particle of Fig. 12(a) is not chiral, unless the dimensions of the top and bottom half crosses are different, whereas the particles in Figs. 12(b), (c) and (d) are all (always) chiral.

The swastika-type particles Figs. 12(b), (c) and (d) can be periodically arranged along the plane of the crosses

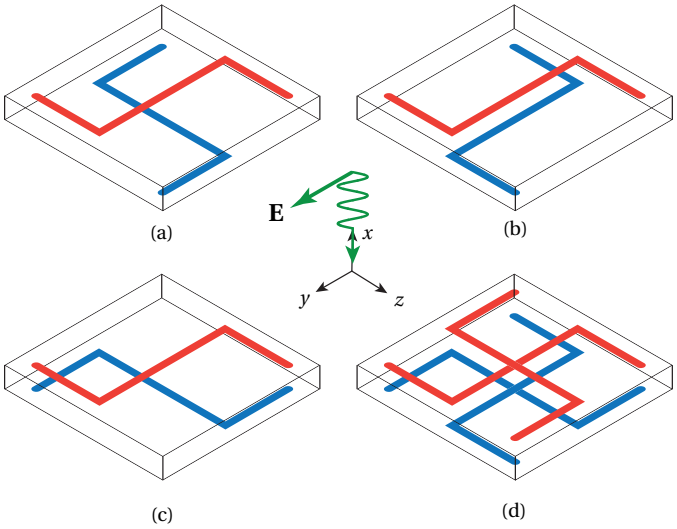

Fig. 12. Swastika-cross two-layer planar metaparticles for chiral metasurfaces. (a) Same-'handedness' $\pi/2$-rotated half crosses (achiral for identical dimensions). (b) Opposite-'handedness' aligned half crosses (chiral). (c) Opposite-'handedness' $\pi/2$-rotated half crosses (chiral). (d) Pair $\pi/2$-rotated full crosses (chiral).

(yz plane in the figure) to form chiral metasurfaces that rotate perpendicularly incident waves. This is shown for the best of the three particles, that Fig. 12(d), in Fig. 13. We see that this particle is essentially equivalent to the twisted Omega or helix particle, and hence also results from the presence of a twisted helix. Due to its $\pi/2$ rotational symmetry, this structure exhibits exactly the same response for field polarization in the perpendicular (z in the figure) direction.

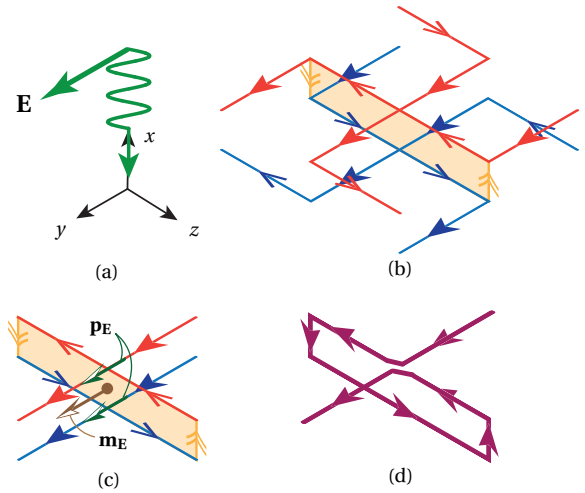

Fig. 13. Response of the swastika metaparticle in Fig. 12(d) (here RH). (a) Polarization and propagation direction of the incident wave. (b) Current induced in the structure from direct excitation (full arrows), conducting current continuity (simple arrows) and displacement current continuity (double arrows). (c) Electric dipole moment (4 side contributions not shown, for simplicity) response ($\mathbf{p}_\mathbf{E}$, corresponding to $\alpha_{\mathrm{ee}}^{yy}$ and χ_{ee}^{yy}) and magnetic dipole moment response ($\mathbf{m}_\mathbf{E}$, corresponding to $\alpha_{\mathrm{me}}^{yy}$ and χ_{me}^{yy}). (d) Equivalent twisted Omega or helix particle [Figs. 5(b) and 9] for this polarization.

The metaparticles of Figs. 12(b) and (c) are much less efficient, in terms of chirality, than that of Fig. 12(d), which is in fact a combination of them. The particle of Fig. 12(b) includes a proper current loop in the z direction for z-polarized waves but fails to provide the required loop for y-polarized waves, while the particle of Fig. 12(c) offers only weak and distorted oblique loops.